

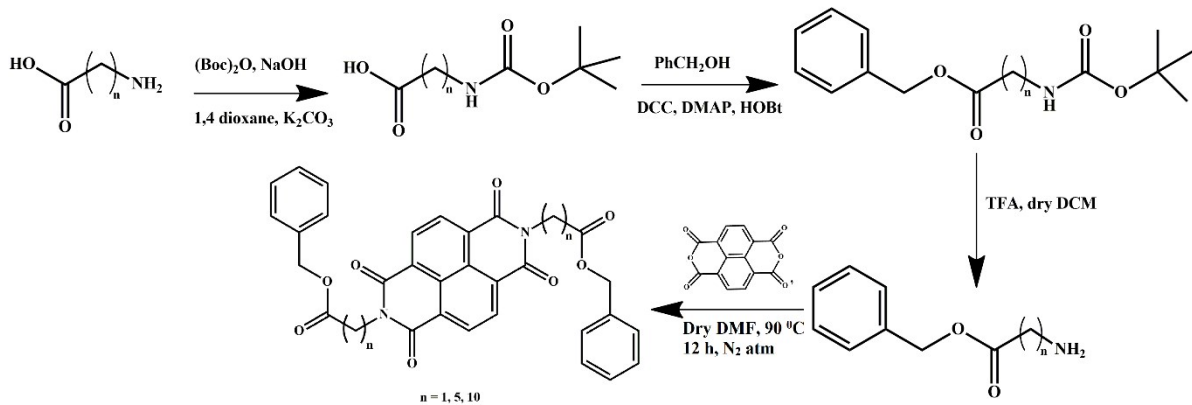
Electronic Supplementary Information (ESI)

Lipase sensing by naphthalene diimide based fluorescent organic nanoparticles: a solvent induced manifestation of self-assembly

Debayan Chakraborty, Deblina Sarkar, Anup Kumar Ghosh and Prasanta Kumar Das*

*School of Biological Sciences, Indian Association for the Cultivation of Science
Jadavpur, Kolkata – 700032, India*

*To whom correspondence should be addressed. E-mail: bcpkd@iacs.res.in



Scheme S1. Synthetic scheme for NDI-based amphiphiles.

Characterization of NDI-1

¹H NMR (500 MHz, CDCl₃, 25 °C, TMS): δ /ppm = 8.75-8.76 (m, 4H, NDI core), 7.40-7.47 (m, 10H, C₆H₅-), 5.06 (s, 4H, -O-CH₂-C₆H₅), 4.28 (s, 4H, NDI-CH₂-C(=O)-O-).

¹³C NMR (400 MHz, CDCl₃): 168.27, 162.78, 141.06, 134.83, 133.15, 128.25, 127.74, 127.19, 121.50, 65.47, 41.54.

MALDI-TOF MS: m/z: 585.53 [M+Na]⁺ (calculated); found = 585.78 [M+Na]⁺.

FTIR: $\delta_{(C=O, \text{ imide})} = 1782 \text{ cm}^{-1}$, $\nu_{(C=O, \text{ imide})} = 1729 \text{ cm}^{-1}$, $\delta_{(C-H)} = 2856 \text{ cm}^{-1}$.

Characterization of NDI-2

¹H NMR (500 MHz, CDCl₃, 25 °C, TMS): δ /ppm = 8.75-8.76 (m, 4H, NDI core), 7.30-7.35 (m, 10H, C₆H₅-), 5.11 (s, 4H, -O-CH₂-C₆H₅), 3.18-3.29 (m, 4H, -CH₂-CH₂-NDI-), 2.38-2.40 (m, 4H, -CH₂-CH₂-C(=O)-O-), 1.73-1.79 (m, 8H, NDI-CH₂-CH₂-CH₂-CH₂-C(=O)-O-), 1.35-1.38 (m, 4H, NDI-CH₂-CH₂-CH₂-CH₂-C(=O)-O-).

¹³C NMR (400 MHz, CDCl₃): 173.48, 162.97, 136.24, 131.11, 128.70, 128.32, 128.30, 126.88, 126.80, 66.30, 40.82, 34.27, 27.86, 26.69, 24.73.

MALDI-TOF MS: m/z: 674.74 [M+Na]⁺ (calculated); found = 697.98 [M+Na]⁺.

FTIR: $\delta_{(C=O, \text{ imide})} = 1785 \text{ cm}^{-1}$, $\nu_{(C=O, \text{ imide})} = 1724 \text{ cm}^{-1}$, $\delta_{(C-H)} = 2854 \text{ cm}^{-1}$.

Characterization of NDI-3

¹H NMR (500 MHz, CDCl₃, 25 °C, TMS): δ /ppm = 8.75-8.76 (m, 4H, NDI core), 7.30-7.35 (m, 10H, C₆H₅-), 5.16 (s, 4H, -O-CH₂-C₆H₅), 3.30-3.40 (m, 4H, -CH₂-CH₂-NDI-), 2.41-2.44 (m, 4H, -CH₂-CH₂-C(=O)-O-), 1.72-1.80 (m, 4H, NDI-CH₂-CH₂-(CH₂)₆-CH₂-C(=O)-O), 1.63-1.67(m, 4H, NDI-CH₂-CH₂-(CH₂)₆-CH₂-CH₂-C(=O)-O), 1.28-1.31 (m, 24H, NDI-CH₂-CH₂-(CH₂)₆-CH₂-CH₂-C(=O)-O-).

¹³C NMR (400 MHz, CDCl₃): 173.87, 159.77, 140.98, 136.23, 133.12, 129.80, 128.78, 127.09, 119.82, 65.35, 40.09, 34.42, 33.78, 32.03, 29.78, 29.44, 29.35, 29.21, 28.99, 26.70.

MALDI-TOF MS: m/z: 815.00 [M+Na]⁺ (calculated); found = 838.21 [M+Na]⁺.

FTIR: $\delta_{(C=O, \text{ imide})} = 1782 \text{ cm}^{-1}$, $\nu_{(C=O, \text{ imide})} = 1717 \text{ cm}^{-1}$, $\delta_{(C-H)} = 2859 \text{ cm}^{-1}$.

Characterization of Intermediate for NDI-2 (OBn-Cap-BOC)

¹H NMR (500 MHz, CDCl₃, 25 °C, TMS): δ/ppm = 7.98 (m, 1H, C₄H₉-C(=O)-O-NH-CH₂-CH₂-CH₂-CH₂-CH₂-), 7.31-7.37 (m, 5H, C₆H₅-), 5.11 (s, 2H, -O-CH₂-C₆H₅), 3.10 (m, 2H, C₄H₉-C(=O)-O-NH-CH₂-CH₂-CH₂-CH₂-CH₂-), 2.34-2.37 (m, 2H, C₆H₅-CH₂-O-C(=O)-CH₂-CH₂-CH₂-CH₂-CH₂-), 1.56-1.68 (m, 4H, C₆H₅-CH₂-O-C(=O)-CH₂-CH₂-CH₂-CH₂-NH-O-), 1.44 (s, 9H, C₄H₉-C(=O)-O-NH-CH₂-CH₂-CH₂-CH₂-CH₂-), 1.34-1.36 (m, 2H, C₄H₉-C(=O)-O-NH-CH₂-CH₂-CH₂-CH₂-CH₂-CH₂-C(=O)C-O-CH₂-C₆H₅). ¹³C NMR (400 MHz, CDCl₃): 173.53, 156.11, 136.22, 128.69, 128.34, 79.57, 66.28, 40.53, 34.09, 29.83, 28.56, 26.43, 24.72.

HRMS: m/z: 321.19 [M]⁺ (calculated); found = 321.22 [M]⁺.

Characterization of Intermediate for NDI-2 (OBn-Cap-NH₂)

¹H NMR (500 MHz, DMSO-d₆, 25 °C, TMS): δ/ppm = 7.31-7.40 (m, 5H, C₆H₅-), 5.09 (m, 2H, H₂N-CH₂-CH₂-CH₂-CH₂-C(=O)-O-), 2.51-2.76 (m, 2H, H₂N-CH₂-CH₂-CH₂-CH₂-C(=O)-O-), 2.347-2.383 (m, 2H, H₂N-CH₂-CH₂-CH₂-CH₂-CH₂-C(=O)-O-), 1.501-1.60 (m, 4H, H₂N-CH₂-CH₂-CH₂-CH₂-C(=O)-O-), 1.26-1.31 (m, 2H, H₂N-CH₂-CH₂-CH₂-CH₂-C(=O)-O-). ¹³C NMR (400 MHz, CDCl₃): 173.64, 130.24, 128.69, 128.33, 66.27, 41.97, 33.95, 27.79, 27.64, 26.45, 24.85.

HRMS: m/z: 221.14 [M]⁺, 244.14 [M+Na]⁺ (calculated); found = 221.19 [M]⁺, 244.14 [M+Na]⁺.

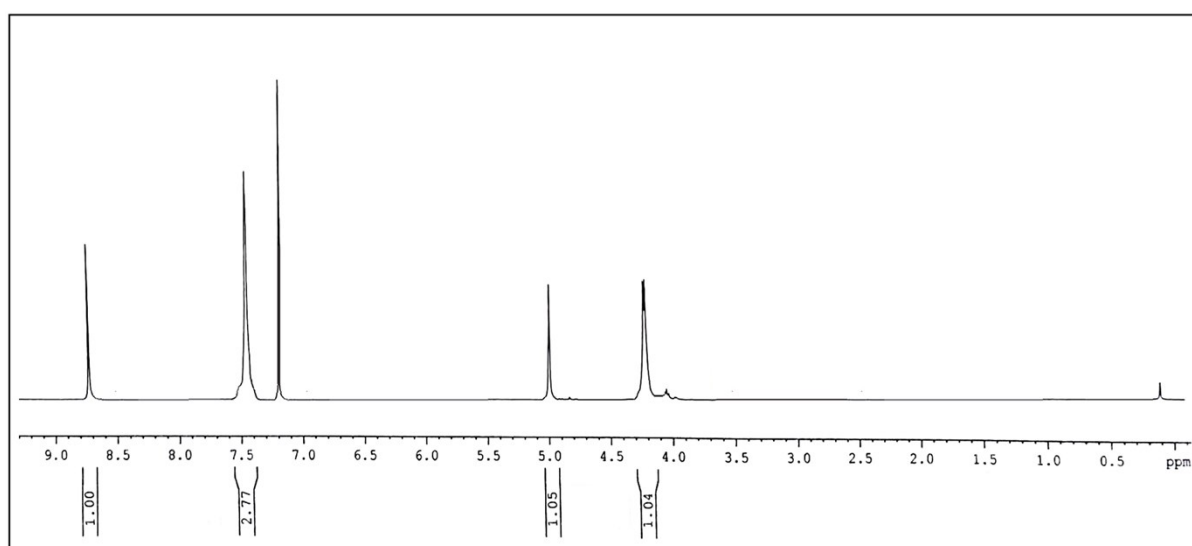


Fig. S1 ¹H NMR spectra of NDI-1.

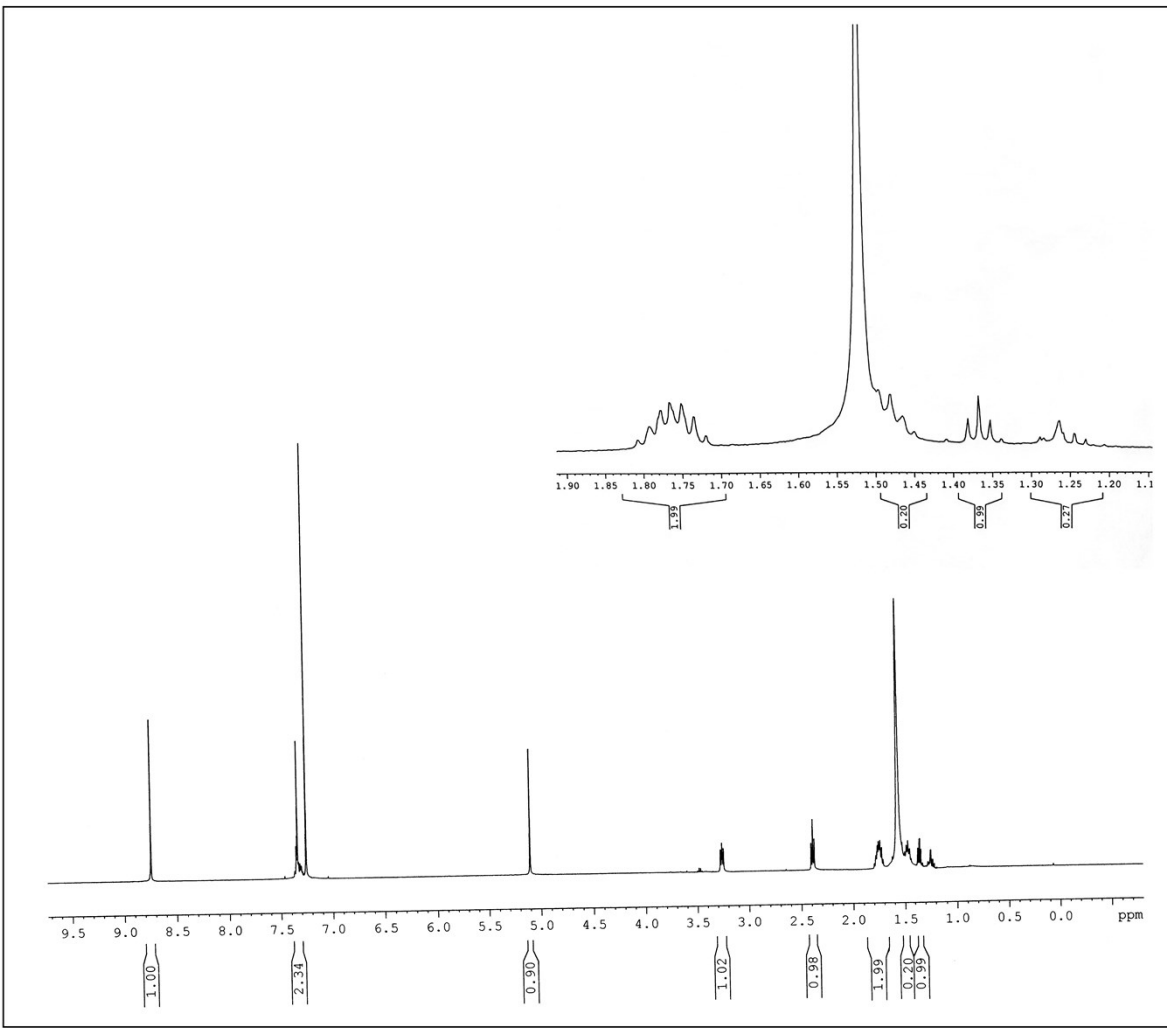


Fig. S2 ¹H NMR spectra of **NDI-2**.

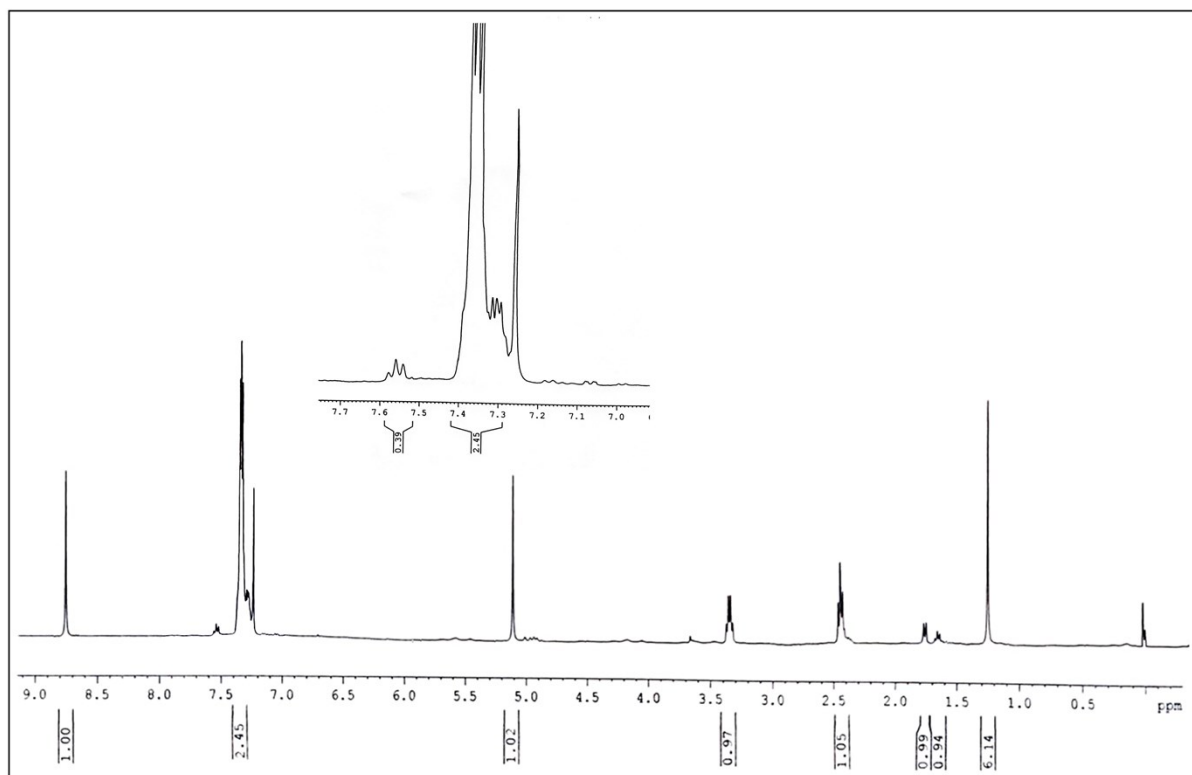


Fig. S3 ¹H NMR spectra of **NDI-3**.

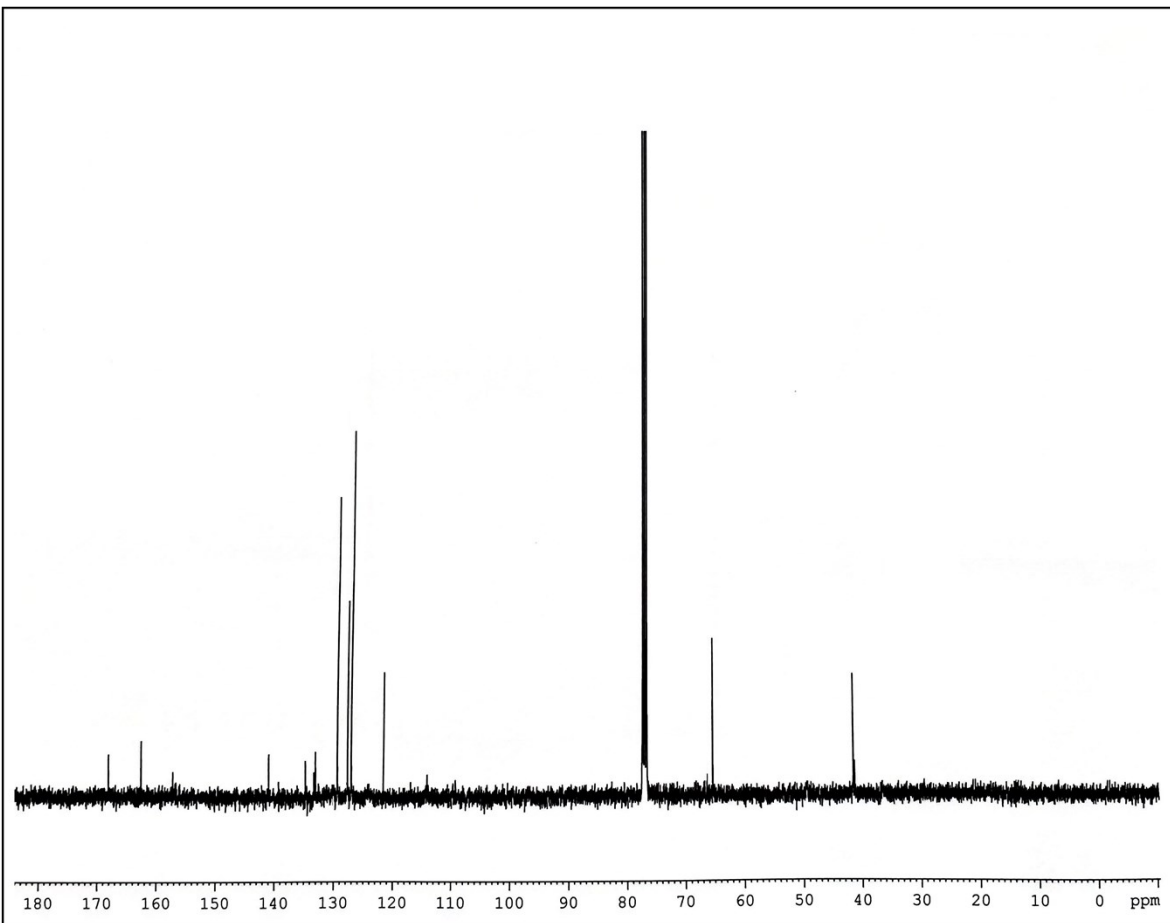


Fig. S4 ^{13}C NMR spectra of **NDI-1**.

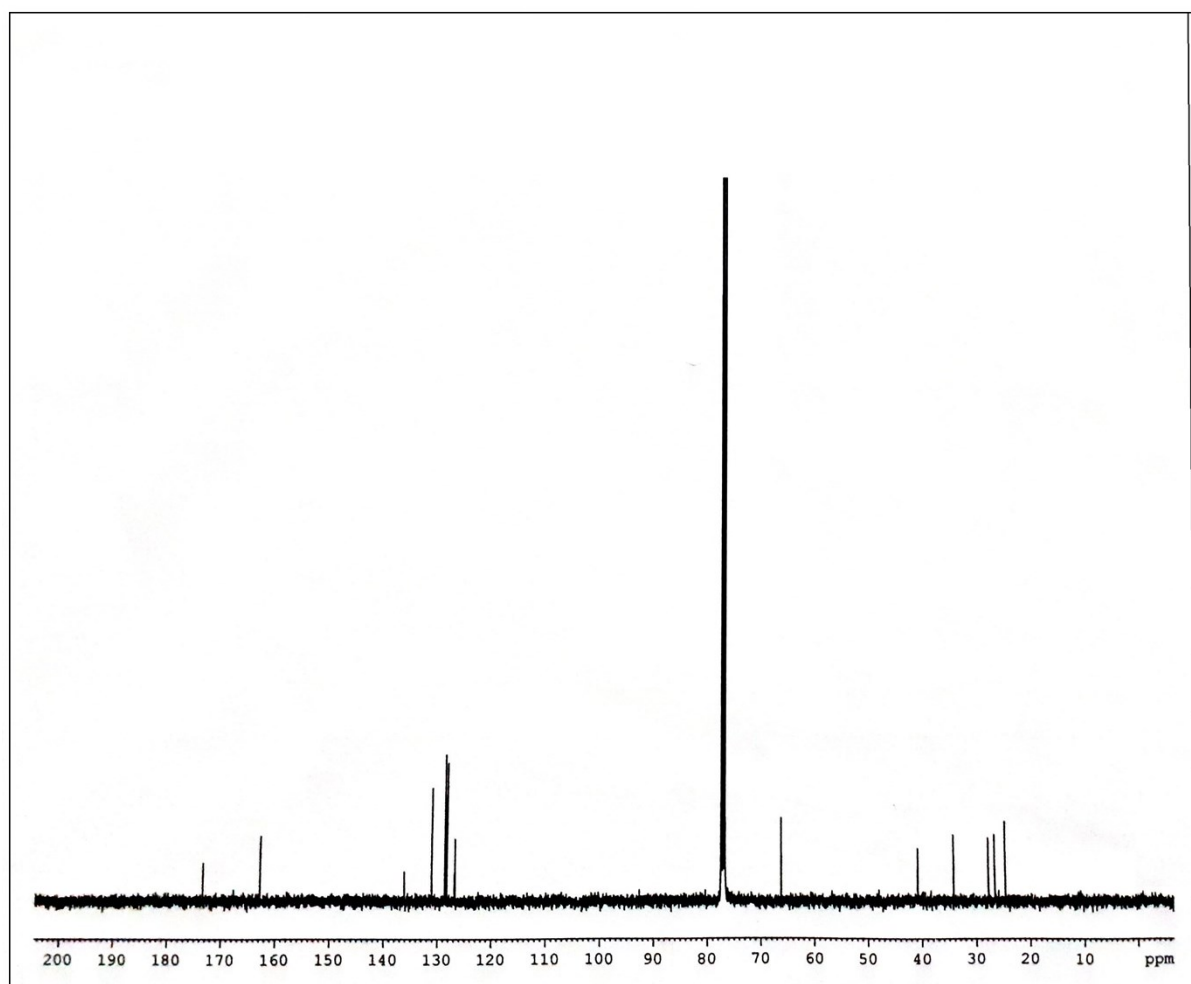


Fig. S5 ^{13}C NMR spectra of **NDI-2**.

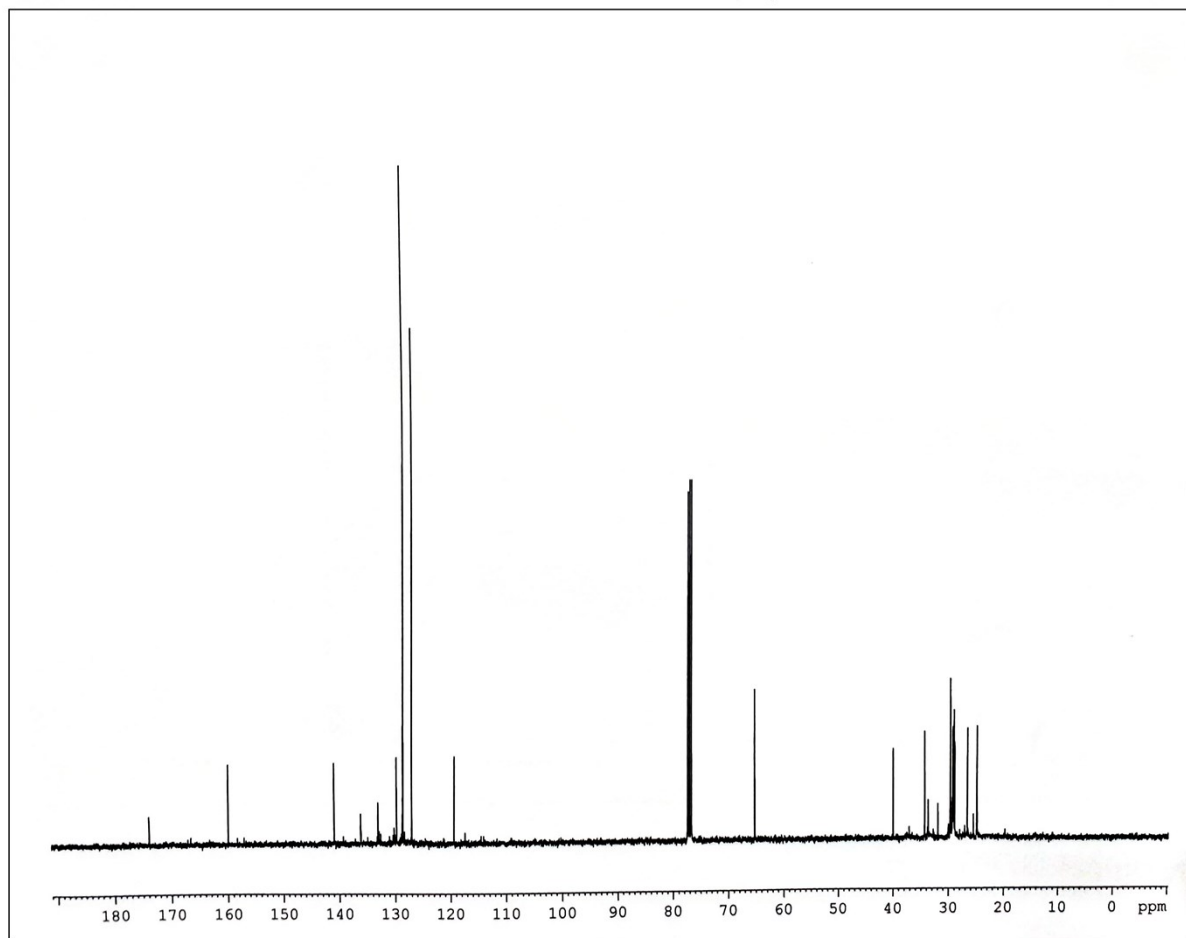


Fig. S6 ¹³C NMR spectra of **NDI-3**.

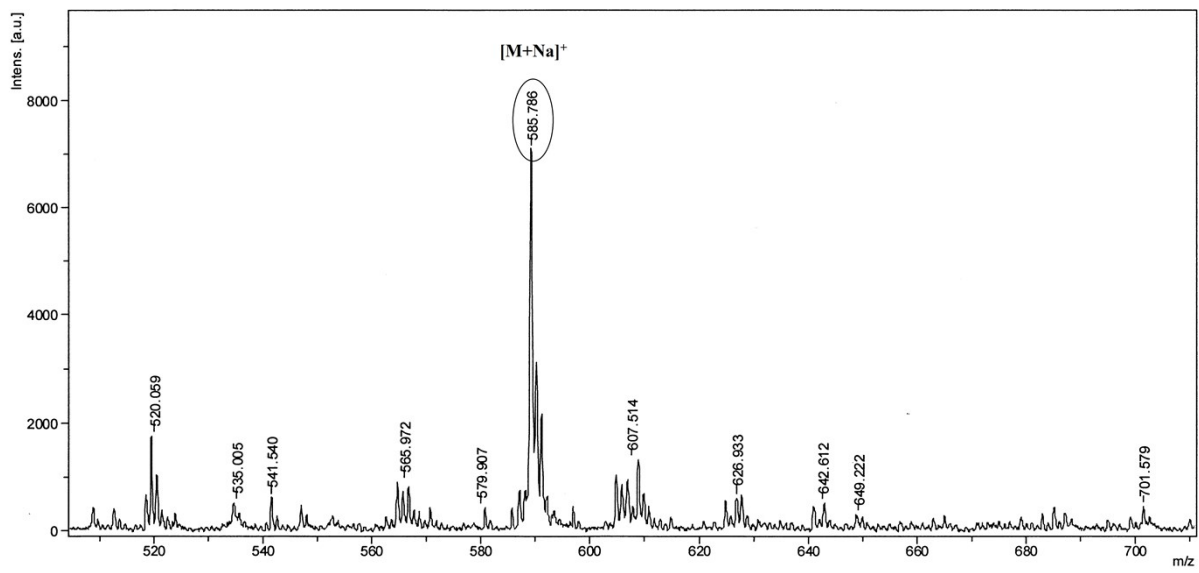


Fig. S7 MALDI-TOF mass spectra of **NDI-1**.

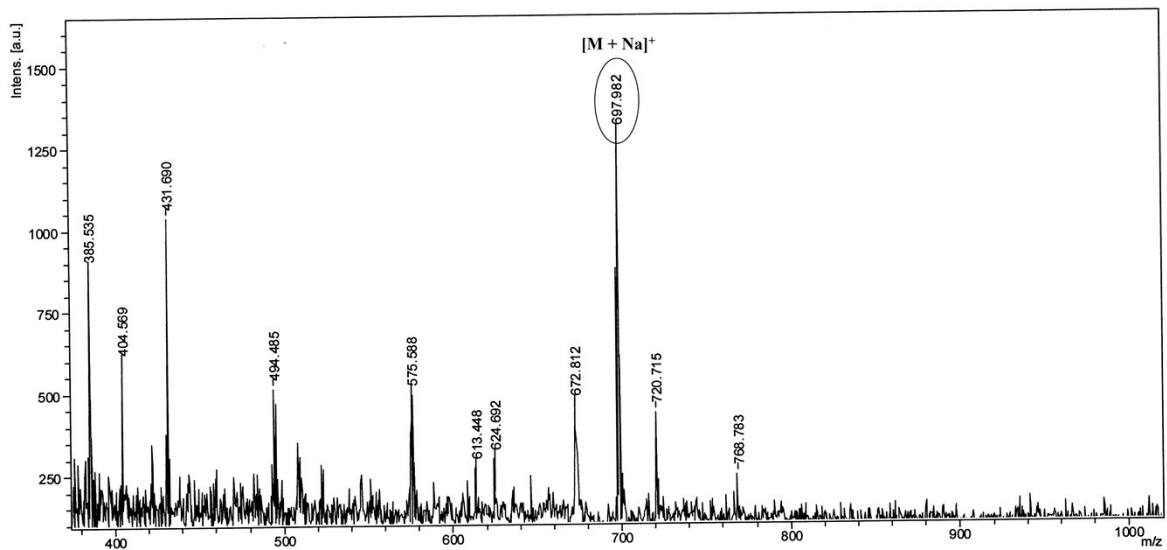


Fig. S8 MALDI-TOF mass spectra of NDI-2.

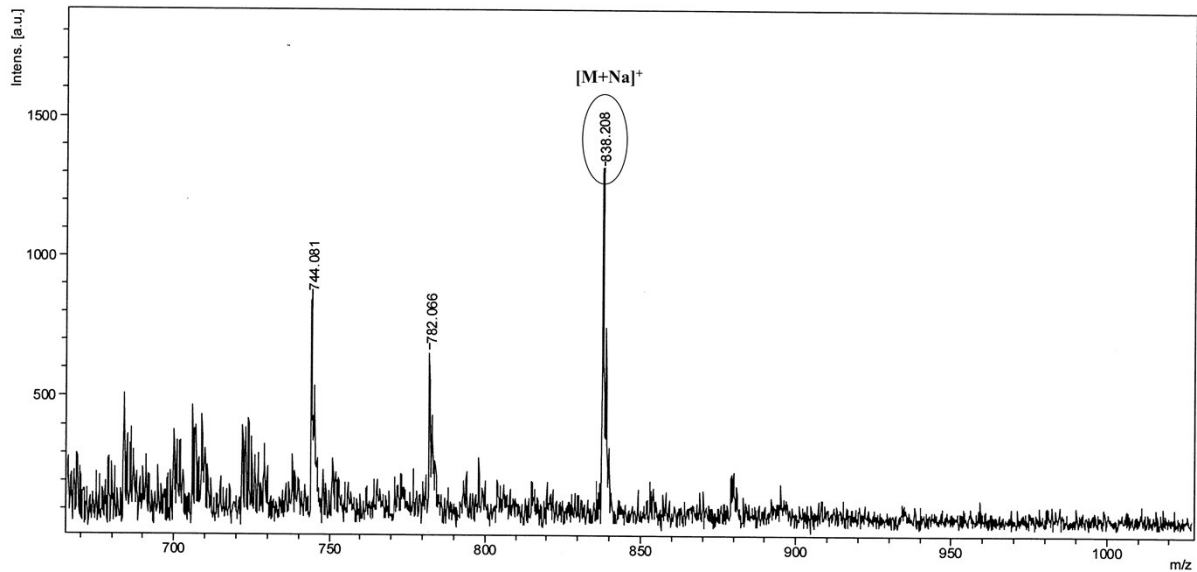


Fig. S9 MALDI-TOF mass spectra of NDI-3.

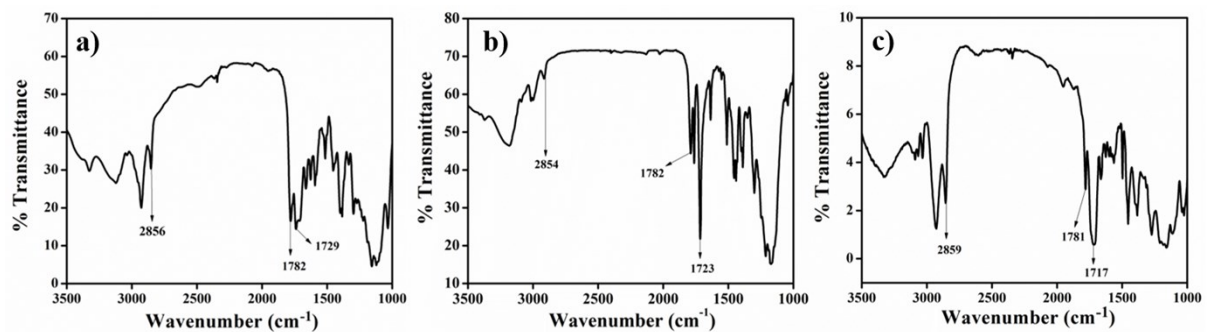


Fig. S10 FT-IR spectra of (a) NDI-1, (b) NDI-2, (c) NDI-3.

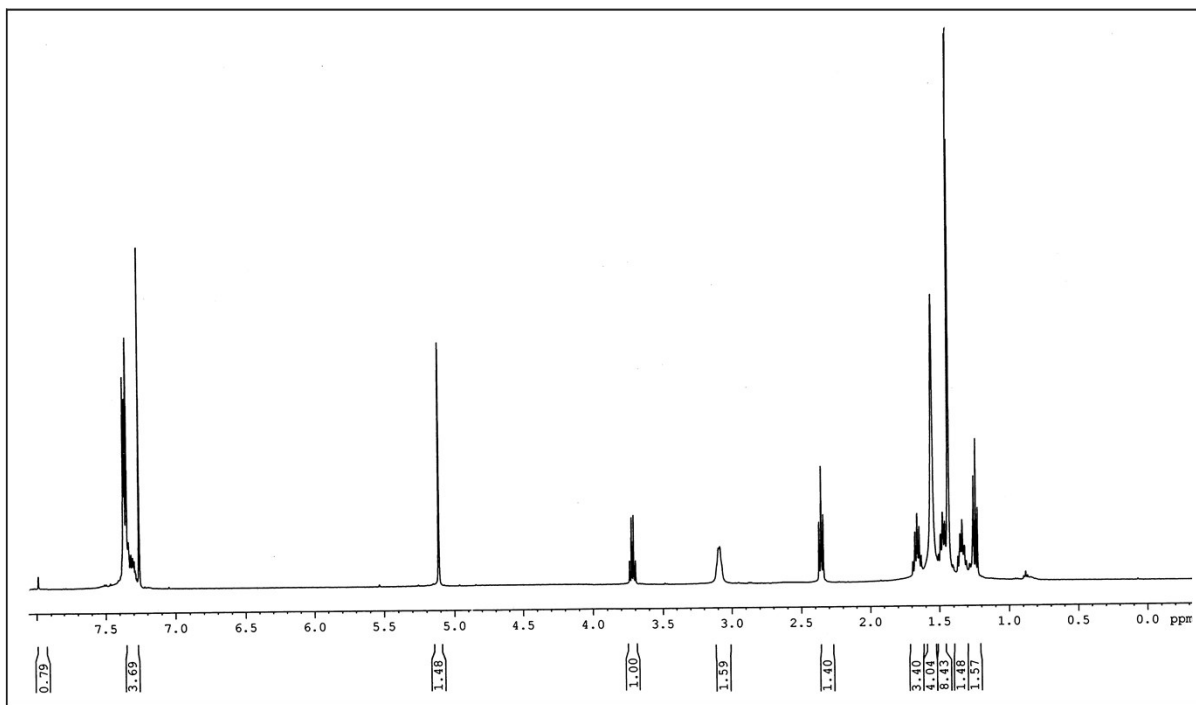


Fig. S11 ¹H-NMR spectra of Boc protected benzyl ester of caproic acid.

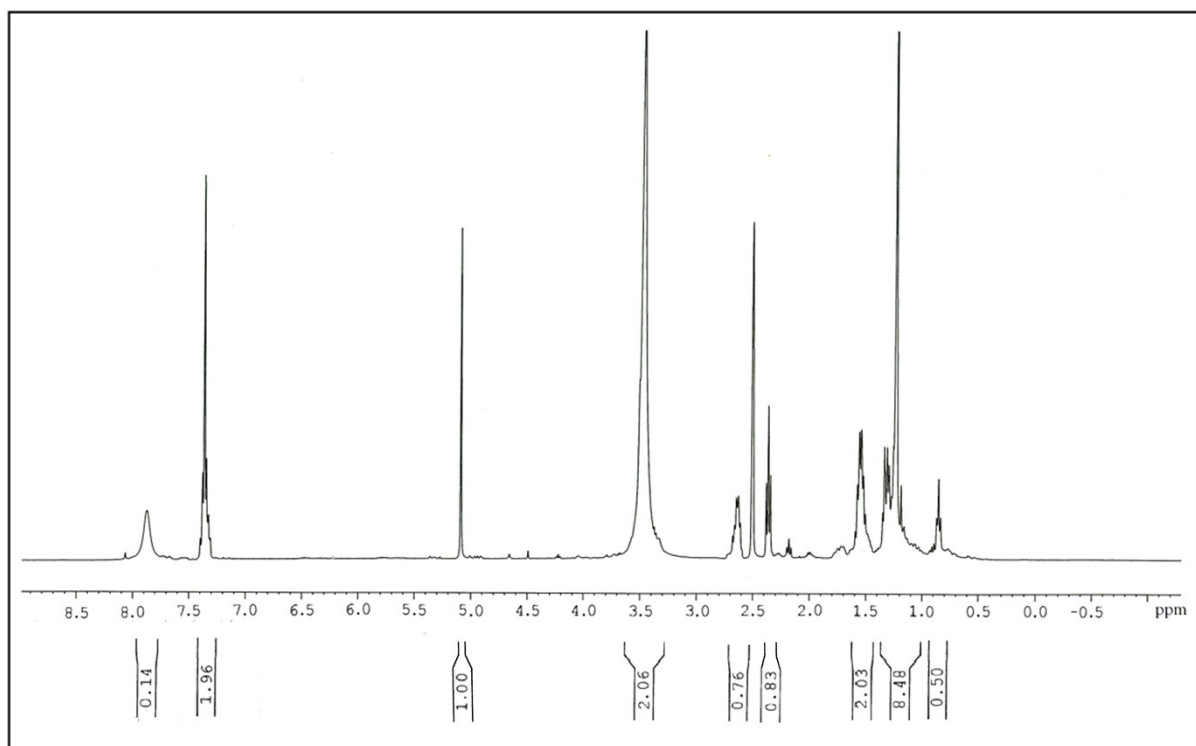


Fig. S12 ¹H-NMR spectra of benzyl ester of caproic acid.

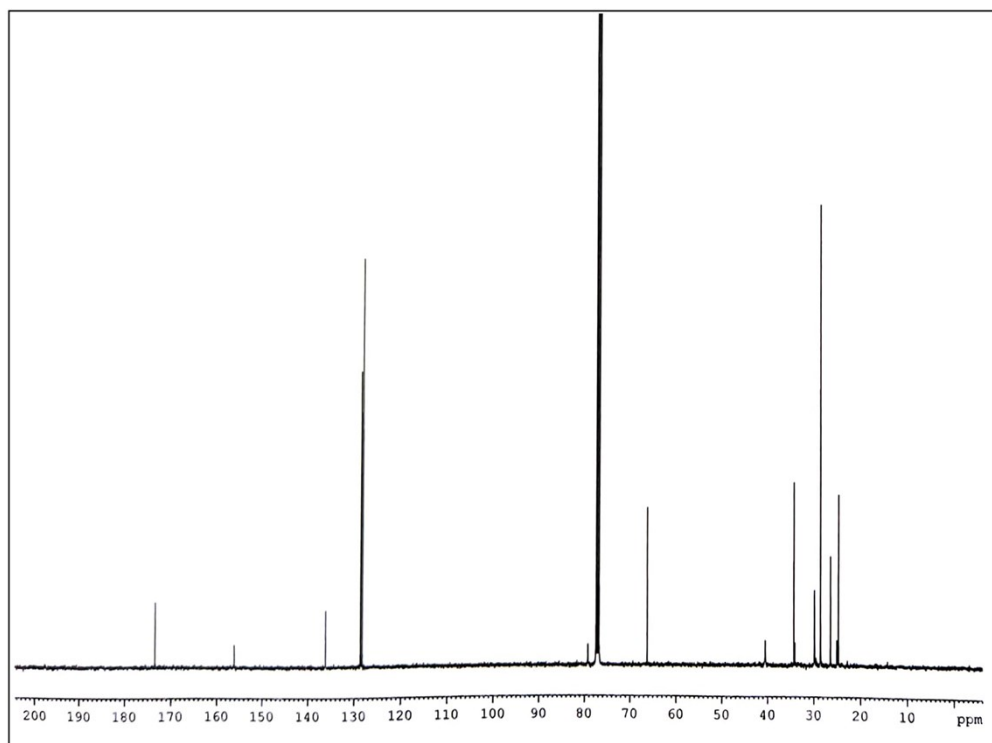


Fig. S13 ¹³C-NMR spectra of Boc protected benzyl ester of caproic acid.

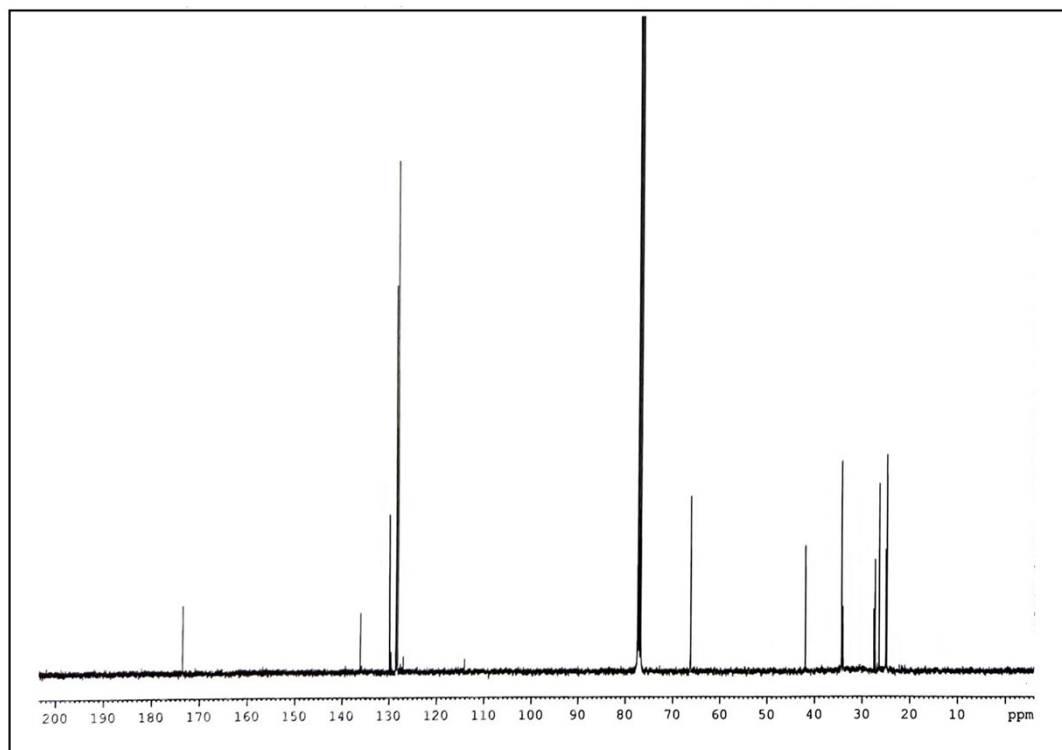


Fig. S14 ¹³C -NMR spectra of benzyl ester of caproic acid.

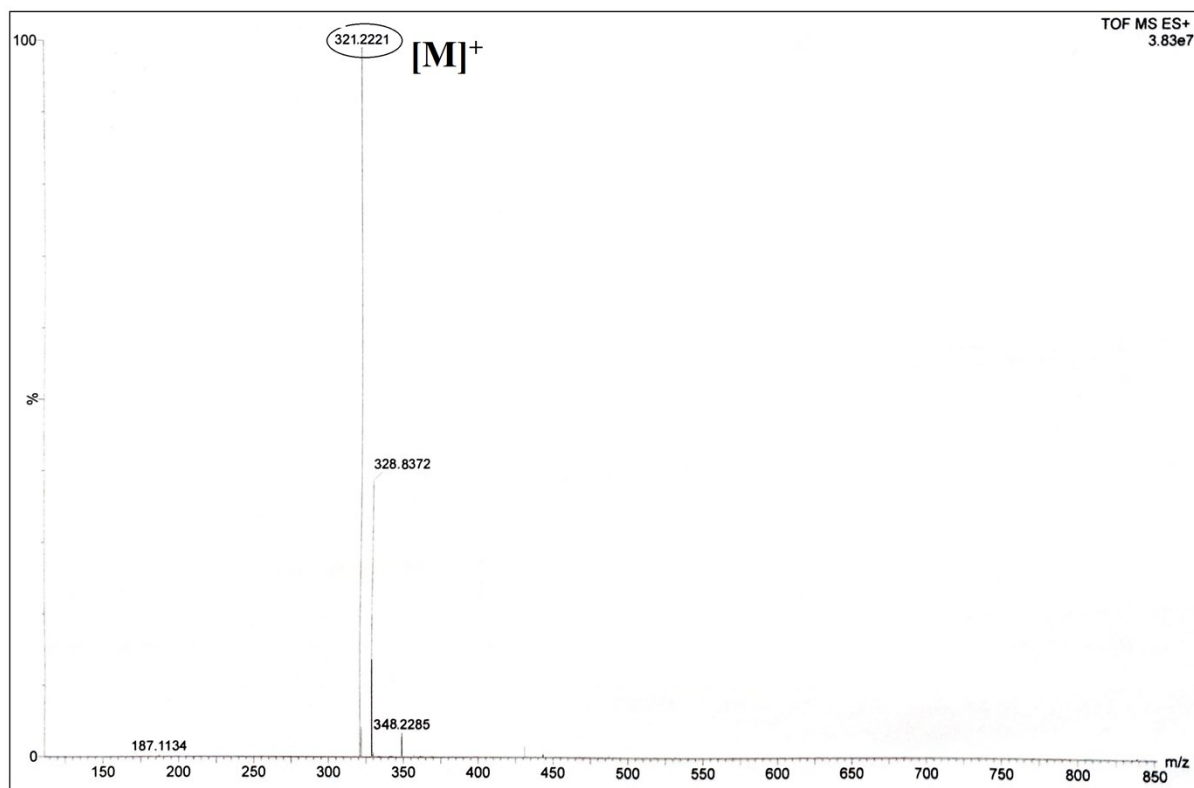


Fig. S15 HRMS spectra of Boc protected benzyl ester of caproic acid.

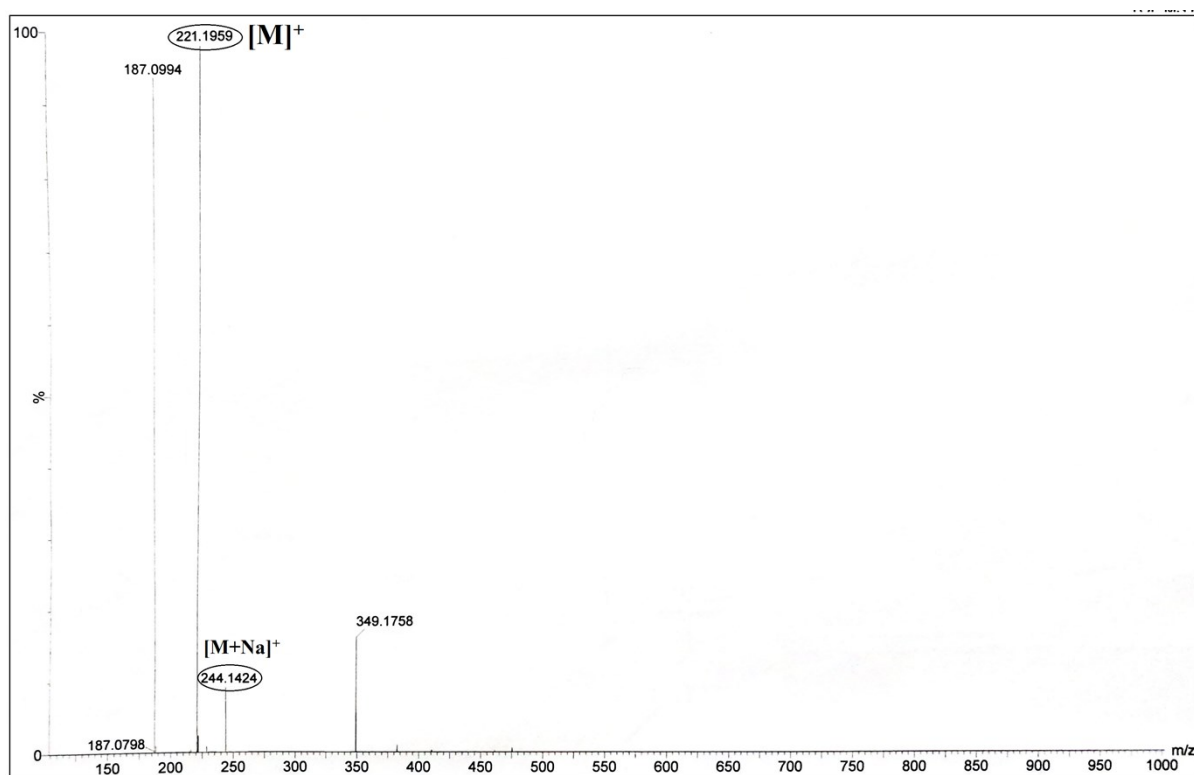


Fig. S16 HRMS spectra of Boc protected benzyl ester of caproic acid.

Table S1 Table for comparison of limit of detection (LOD) of different lipase sensing probes.

Probes	LOD	Response type	References
Tetraphenylethylene (TPE) derivative (TPE-COO _{C₆H₁₃})	0.1 mg mL ⁻¹	Fluorescence Turn On	<i>Sens. Actuators, B</i> 2017 , 238, 765-771.
Tetraphenylethylene (TPE) derivative (TPE-Glutamic acid)	0.13 U L ⁻¹	Fluorescence Turn On	<i>Chem. Sci.</i> 2017 , 8, 6188-6195.
Tetraphenylethylene (TPE) derivative (TPE- γ -cyclodextrin)	0.11 U L ⁻¹	Fluorescence Turn On	<i>Chem. Comm</i> 2019 , 55, 6417-6420.
4-cyano-4'-pentylbiphenyl based liquid crystal	0.01 μ g mL ⁻¹	Structural changes in whispering gallery mode and wavelength shift	<i>Analyst</i> , 2020 , Advance Article. (https://doi.org/10.1039/D0AN01187H)
4-cyano-4'-pentylbiphenyl based liquid crystal droplet	0.1 μ g mL ⁻¹	Structural changes of liquid droplets	<i>Liquid Crystals</i> , 2014 , 41, 597-602.
Reduced graphene oxide base chemiresistor	6.087 U L ⁻¹	Voltage change in the designed circuit	<i>IEEE Sens. Lett.</i> 2018 , 2, 1-4.
Gold Nanorods (AUNRs)	0.017 mg mL ⁻¹	colorimetric assay	<i>Anal. Methods</i> , 2019 , 11, 2286-2291.
CdSe, ZnS based QDs ratiometrically self-assembled with ester-containing peptidyl substrate conjugates	0.0002 U	Förster resonance energy transfer	<i>ACS Sens.</i> 2020 , 5, 1295-1304.
Surface Acoustic Wave Sensor System	13 U L ⁻¹	Conductance measurement	<i>Anal Biochem.</i> 1995 , 226, 207-211
Naphthalene diimide derivative	10.0±0.8 μg L⁻¹	Fluorescent Turn Off	Present Study

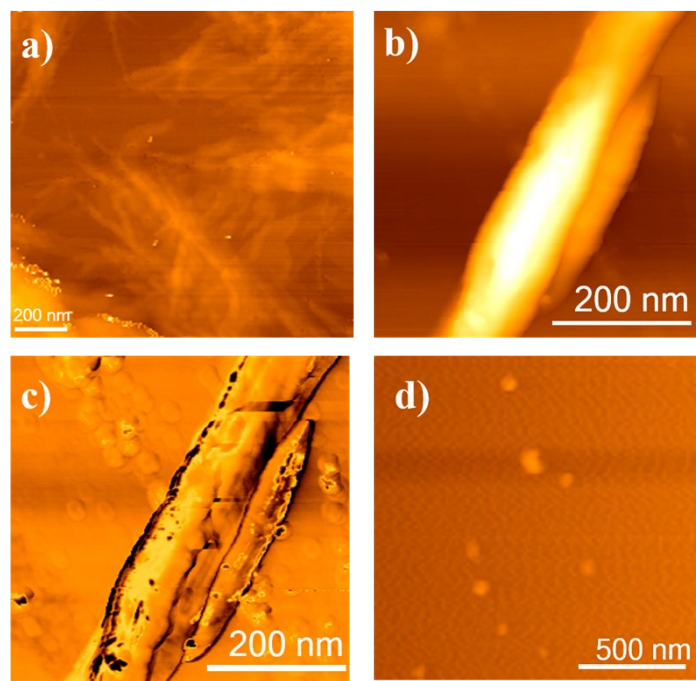


Fig. S17 AFM image of **NDI-2** ($[NDI-2] = 20 \mu M$) (a) in (70:30, v/v); (b) AFM image (phase), (c) AFM image (topography) in (50:50, v/v); (d) in (1:99, v/v) DMSO-water binary solvent mixture.

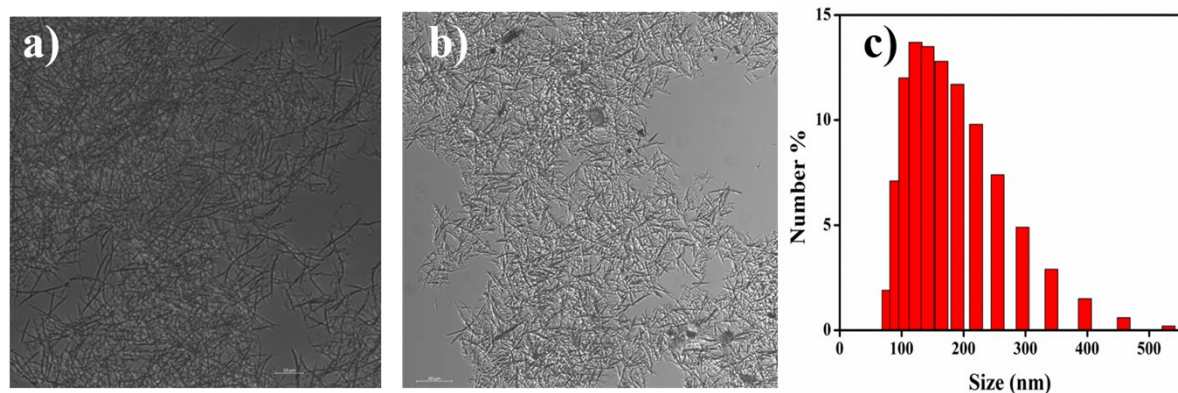


Fig. S18 Bright field images **NDI-2** in (a) (70:30, v/v), (b) (50:50, v/v) DMSO-water binary solvent mixture, (c) DLS plot of particles size distribution of **NDI-2** in (1:99, v/v) DMSO-water binary solvent mixture ($[NDI-2] = 20 \mu M$).

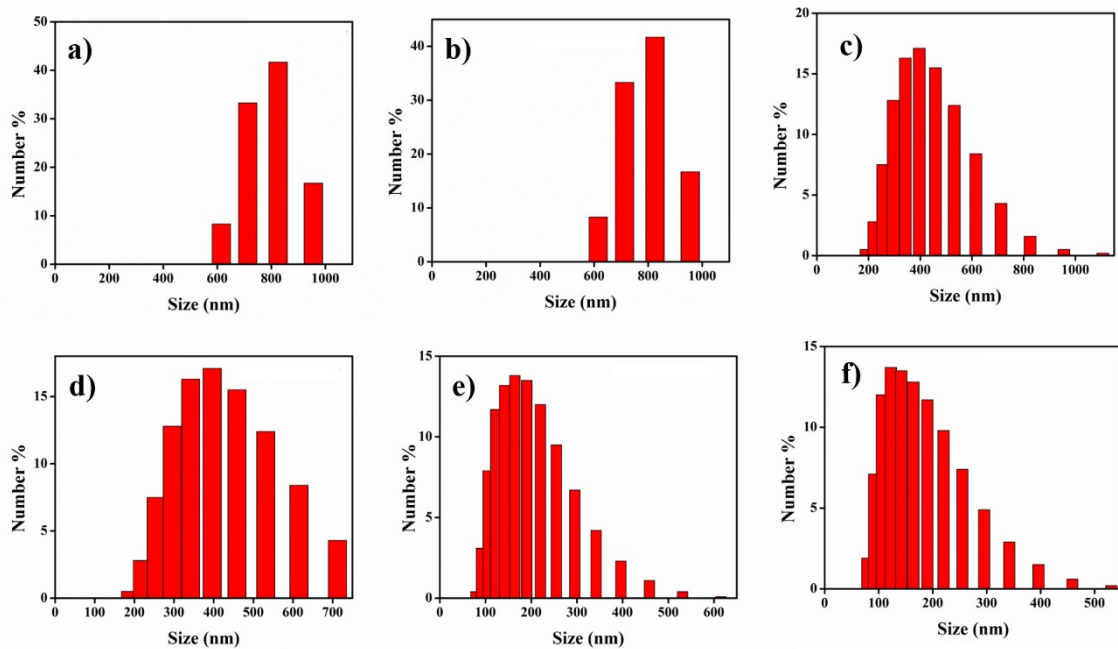


Fig. S19 DLS measurement of **NDI-2** (20 μM) in a) 50:50 v/v, b) 40:60 v/v c) 30:70 v/v, d) 20:80 v/v, e) 10:90 v/v, f) 1:99 v/v DMSO-water solvent composition.

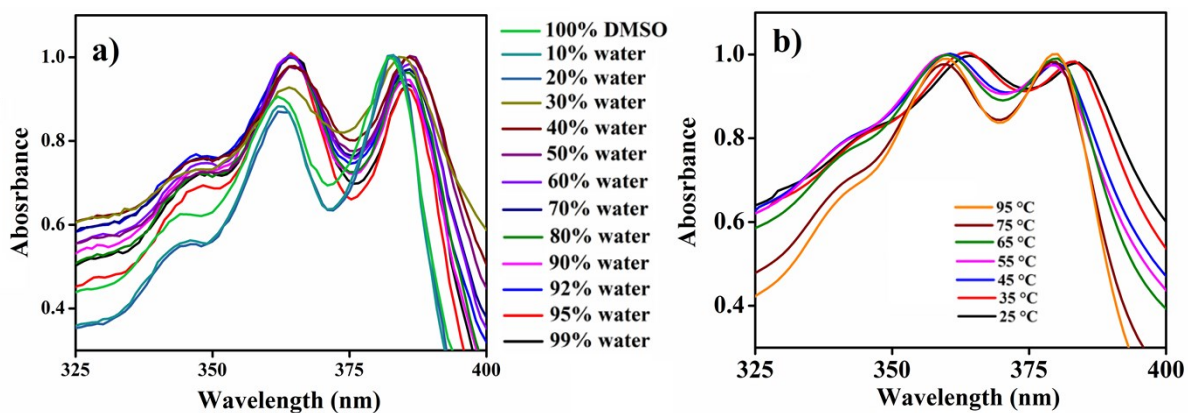


Fig. S20 (a) Normalised UV-Visible spectra of **NDI-2** (20 μM) in varying DMSO-water solvent mixtures. (b) Normalised temperature dependent UV-visible spectra of **NDI-2** (25 μM) in 1:99 v/v, DMSO-water.

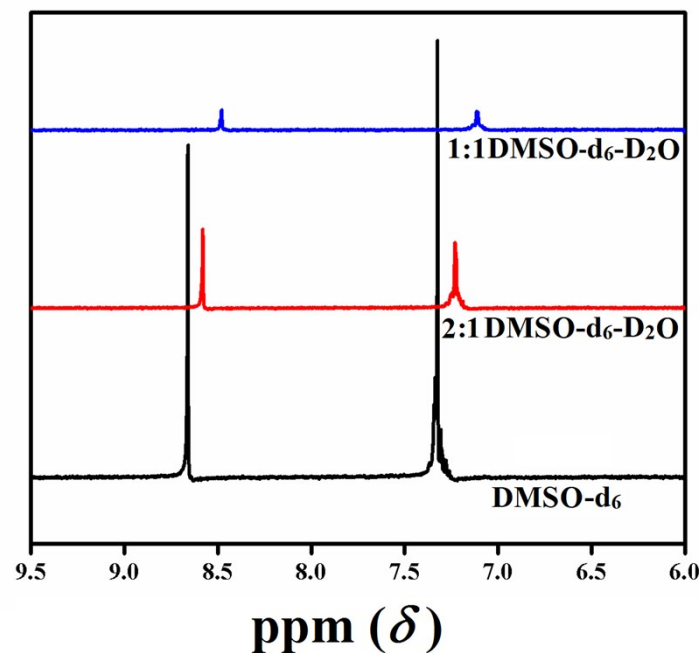


Fig. S21 Solvent dependent ^1H -NMR of **NDI-2** from non-self-assembled state (in DMSO-d_6) to self-assembled state ($\text{DMSO-d}_6\text{-D}_2\text{O}$).

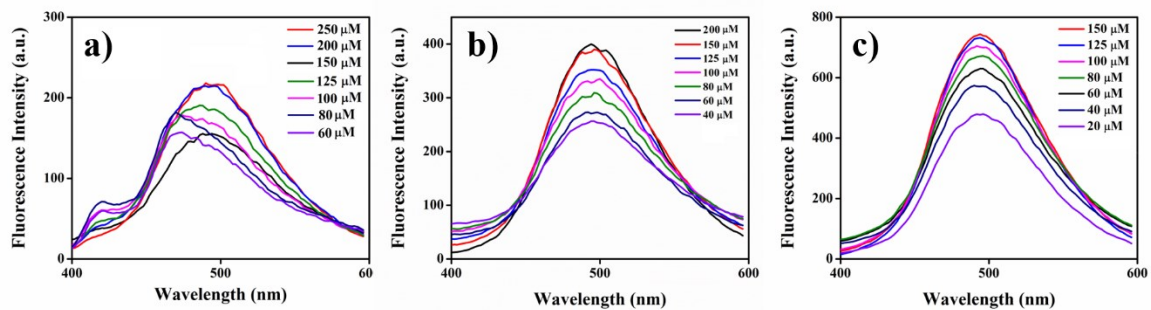


Fig. S22 Concentration-dependent emission spectra of **NDI-2** at different fraction of water (f_{w}): (a) $f_{\text{w}} = 30 \text{ vol\%}$, (b) $f_{\text{w}} = 50 \text{ vol\%}$, (c) $f_{\text{w}} = 99 \text{ vol\%}$.

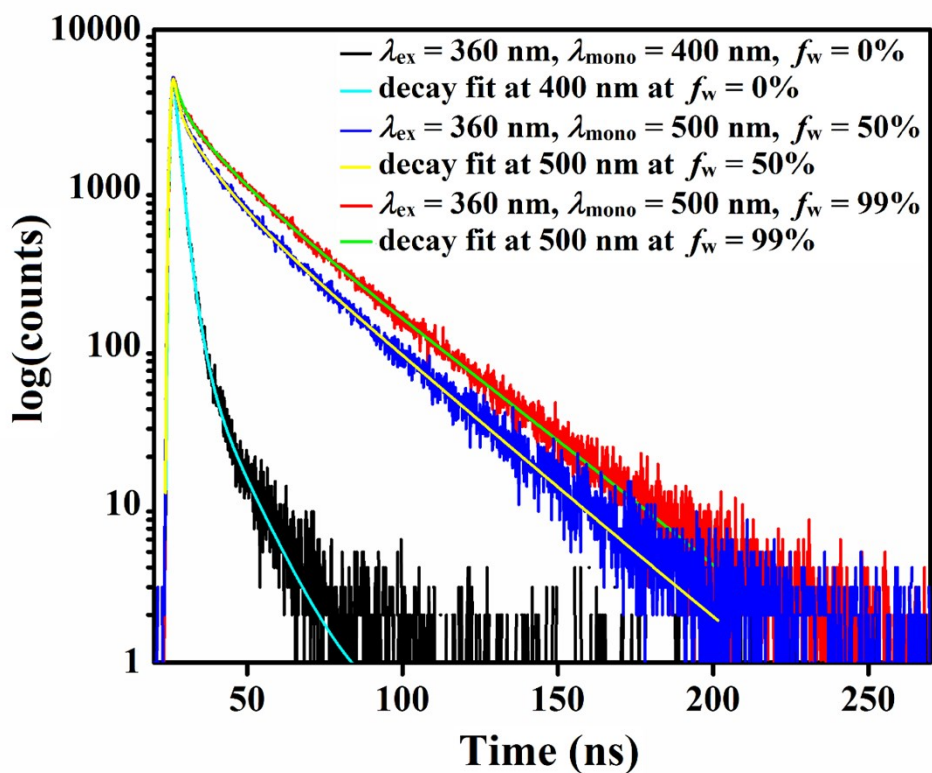


Fig. S23 TCSPC decay profile of NDI-2 with 360 nm excitation in different solvent compositions of DMSO-water.

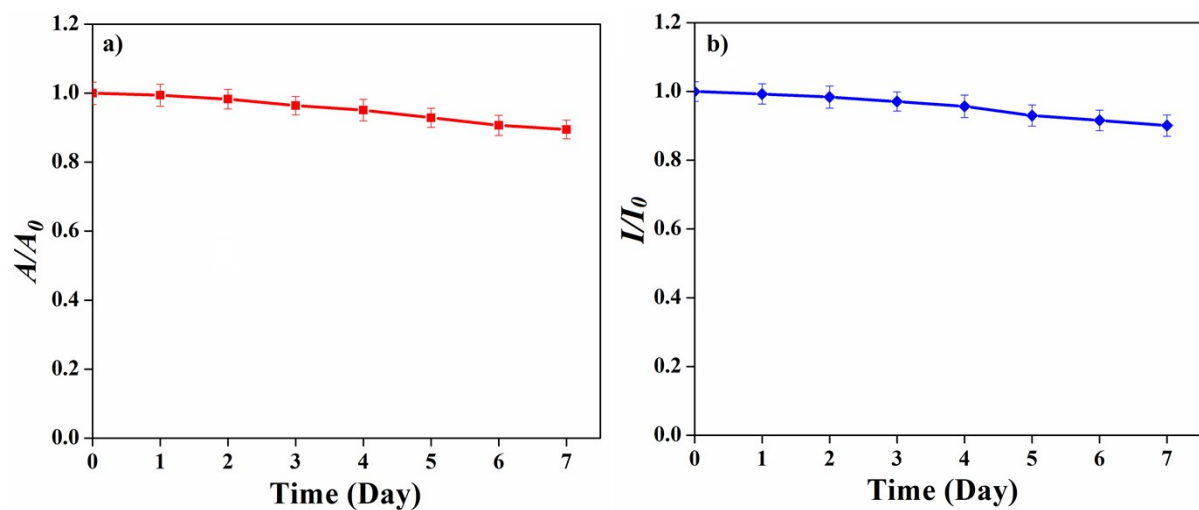


Fig. S24 Ratio of (a) absorbance value, (b) fluorescence intensity over time for NDI-2 FONP at $f_w = 99$ vol% in DMSO.

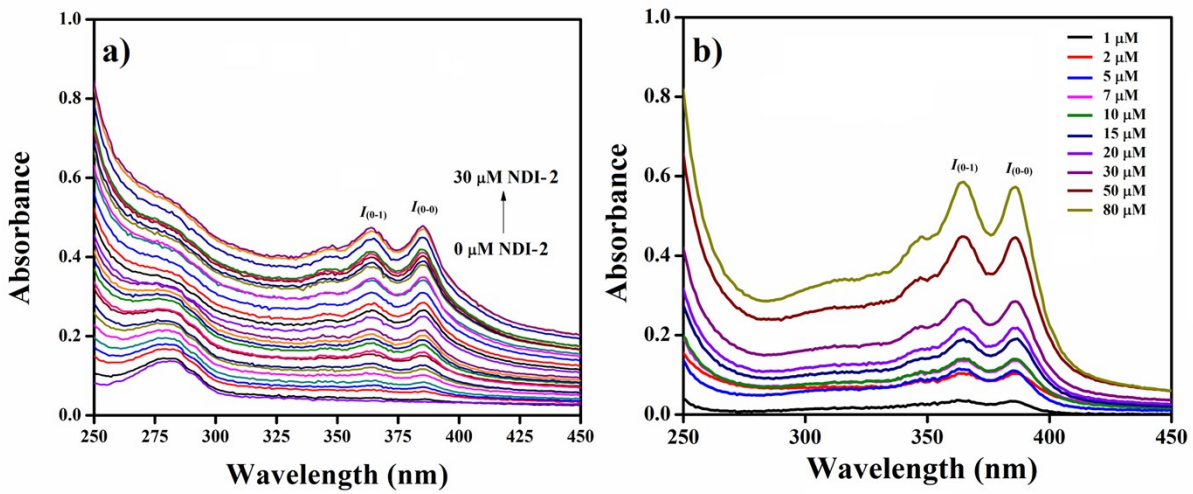


Fig. S25 UV-vis spectra of **NDI-2** (0-30 μM) in (a) presence of 0.5 mg L^{-1} CV lipase and (b) absence of lipase.

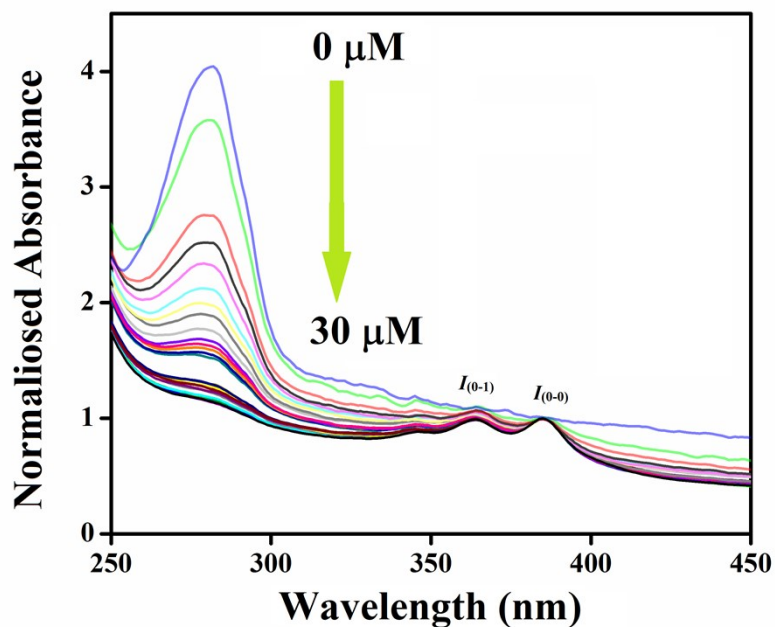


Fig. S26 Normalised (with respect to 385 nm) UV-vis spectra of **NDI-2** (0-30 μM) in presence of 0.5 mg L^{-1} CV lipase.

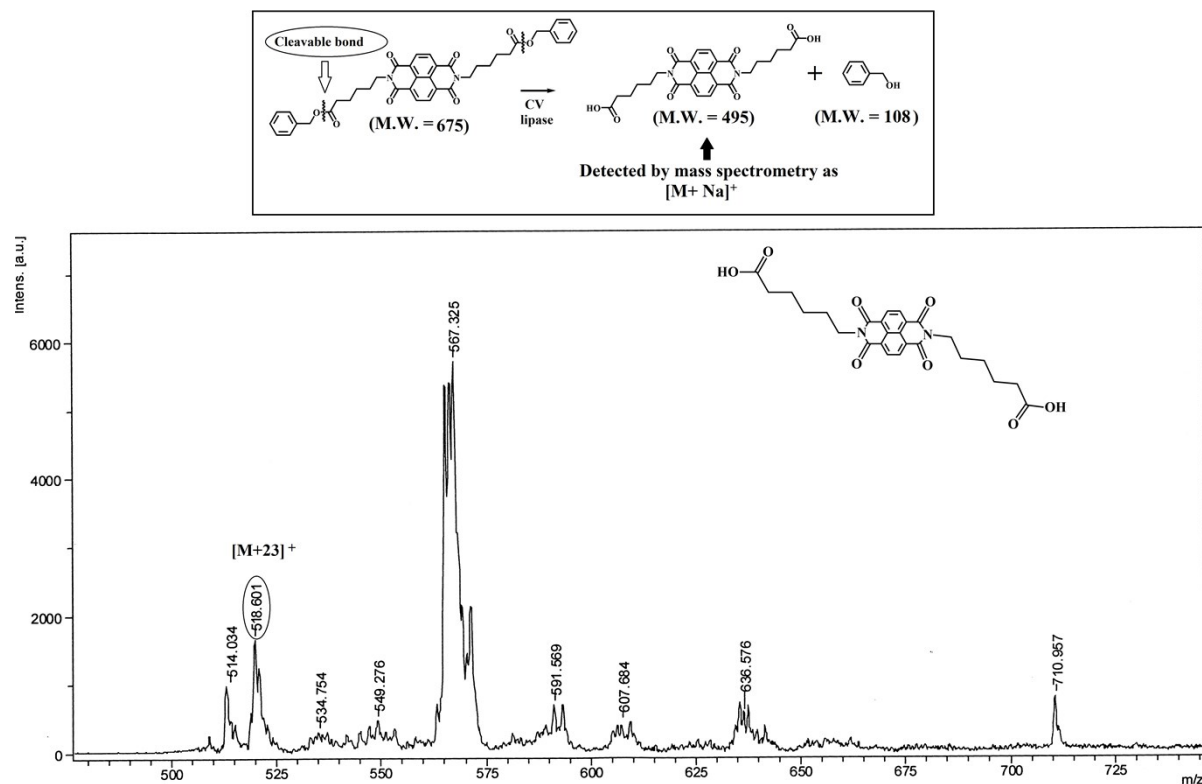


Fig. S27 Mass Fragment of **NDI-2** after treatment with CV lipase.

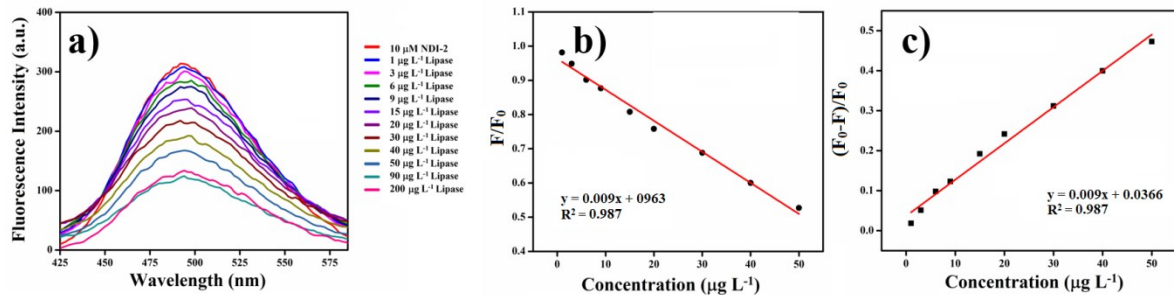


Fig. S28 (a) Fluorescence spectra of **NDI-2** FONPs (10 μM) in absence and presence of varying concentration of CV lipase (excitation wavelength =350 nm), (b) Stern-Volmer plot of CV lipase doped in (1:99, v/v) DMSO-water solution of **NDI-2** (10 μM), (c) fluorescence response of **NDI-2** FONPs towards CV lipase sensing with varying concentration of lipase in (1:99, v/v) DMSO-water ($[\text{NDI-2}] = 10 \mu\text{M}$).

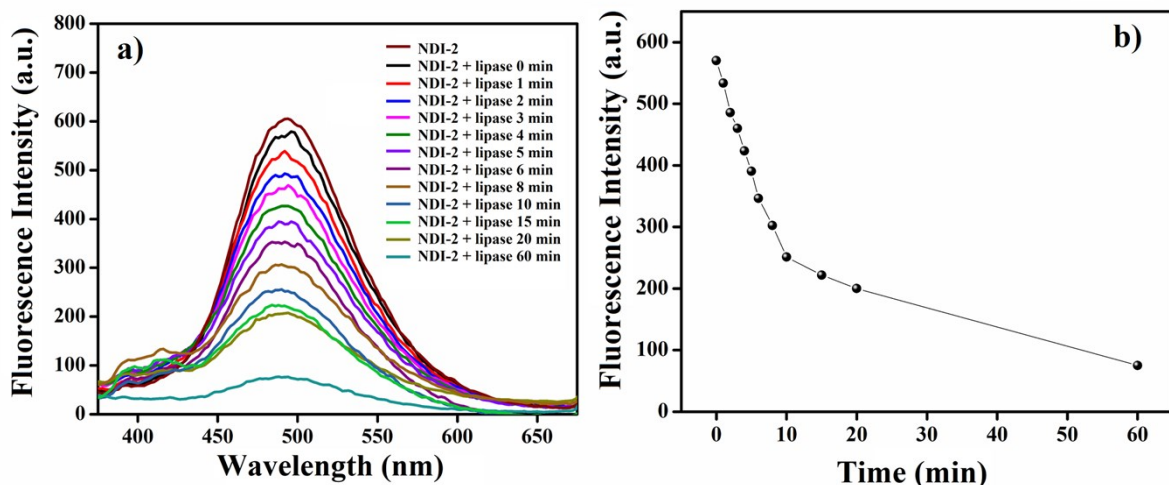


Fig. S29 (a) Time dependent fluorescence spectra of **NDI-2** in (1:99, v/v) DMSO-water solution doped with CV lipase. (b) Variation of fluorescence Intensity of **NDI-2** in (1:99, v/v) DMSO-water doped with CV lipase with time.

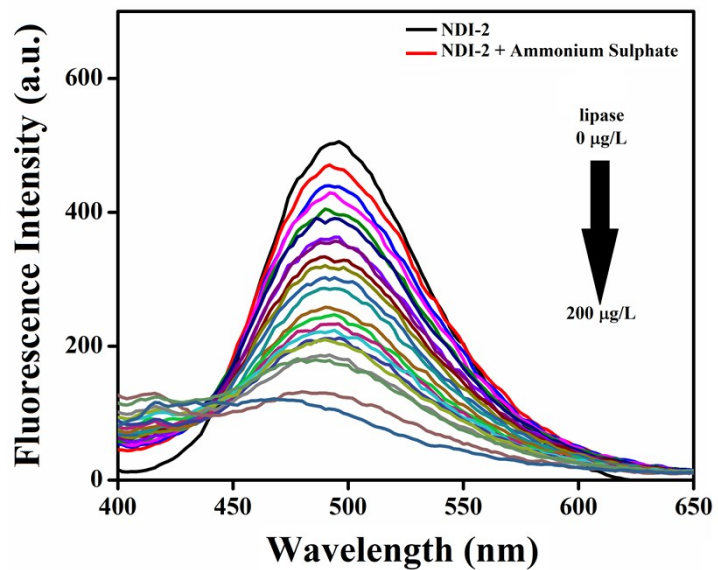


Fig. S30 Fluorescence spectra of **NDI-2** FONPs (25 μM) in presence of varying concentration of CV lipase (excitation wavelength = 350 nm) and ammonium sulphate (25 μM).

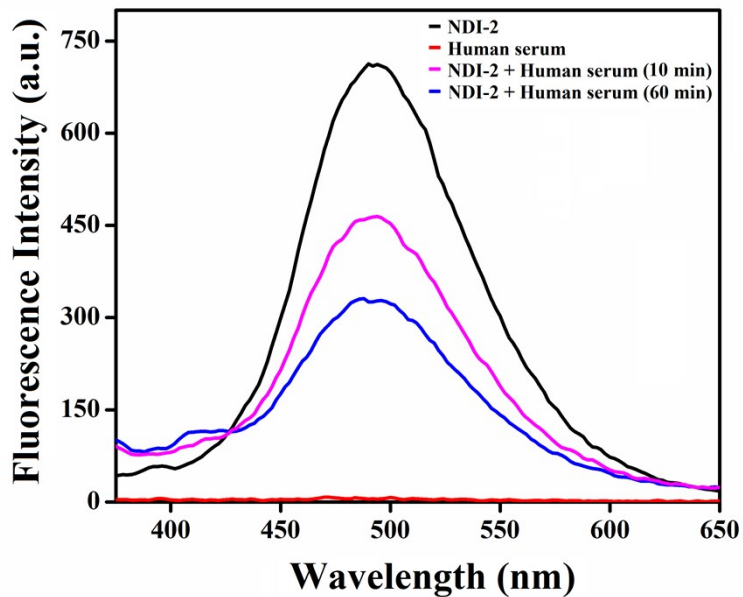


Fig. S31 Fluorescence spectra of **NDI-2** FONPs prepared from (1:99, v/v) DMSO-water in presence of diluted human serum.